



## Abstract

Although laboratory studies show that biogenic volatile organic compounds (VOCs) yield substantial secondary organic aerosol (SOA), production of biogenic SOA as indicated by upward fluxes has not been conclusively observed over forests. Further, while aerosols are known to deposit to surfaces, few techniques exist to provide chemically-resolved particle deposition fluxes. To better constrain aerosol sources and sinks, we have developed a new technique to directly measure fluxes of chemically-resolved submicron aerosols using the high-resolution time-of-flight aerosol mass spectrometer (HR-AMS) in a new, fast eddy covariance mode. This approach takes advantage of the instrument's ability to quantitatively identify both organic and inorganic components, including ammonium, sulphate and nitrate, at a temporal resolution of several Hz. The new approach has been successfully deployed over a temperate ponderosa pine plantation in California during the BEARPEX-2007 campaign, providing both total and chemically resolved non-refractory (NR) PM<sub>1</sub> fluxes. Average deposition velocity for total NR-PM<sub>1</sub> aerosol at noon was  $2.05 \pm 0.04$  mm/s. Using a high resolution measurement of the NH<sub>2</sub><sup>+</sup> and NH<sub>3</sub><sup>+</sup> fragments, we demonstrate the first eddy covariance flux measurements of particulate ammonium, which show a noon-time deposition velocity of  $1.9 \pm 0.7$  mm/s and are dominated by deposition of ammonium sulphate.

## 1 Introduction

Aerosols affect air quality (Martin et al., 2003; Monks et al., 2009), human health (Dominici et al., 2006; Brook et al., 2010) and climate (Solomon et al., 2007; Isaksen et al., 2009), but remain a poorly understood component of the Earth's atmosphere. Dry deposition is an important aerosol sink, influencing particle lifetime. Models currently calculate deposition with parameterizations that have not been sufficiently tested in the real-world (Wesely et al., 2000) leading to significant differences in the particle loss rates predicted by different models (Textor et al., 2006). Better measurements and

AMTD

3, 5867–5905, 2010

### Eddy covariance HR-AMS aerosol fluxes

D. K. Farmer et al.

Title Page

Abstract

Introduction

Conclusions

References

Tables

Figures

⏪

⏩

◀

▶

Back

Close

Full Screen / Esc

Printer-friendly Version

Interactive Discussion



parameterizations of aerosol deposition rates are important for more accurate aerosol modeling (Kanakidou et al., 2005). Further, deposition of gas-phase semi-volatile organic compounds is poorly constrained, and ignoring it may cause up to 50% overestimation of secondary organic aerosol (SOA) in chemical transport models (Bessagnet et al., 2010).

The rate of aerosol movement across the surface-atmosphere interface, or aerosol flux, affects not only aerosol lifetime and atmospheric chemistry, but also surface chemistry, particularly when the surface is a forest. Particulate deposition to ecosystems can be a major nutrient source, affecting nitrogen, phosphorus and calcium cycling (e.g., Lindberg et al., 1986; Pett-Ridge, 2009; Vicars et al., 2010). Nitrogen is a key component of both anthropogenic and biogenic aerosols, and is often a limiting nutrient in temperate forests (Vitousek et al., 1991), the supply of which can stimulate plant growth and carbon storage in forests (Magnani et al., 2007; Sutton et al., 2008). High nitrogen fertilization levels, however, can reduce forest health and cause plant death and loss of diversity (Matson et al., 2002; Magill et al., 2004; Stevens et al., 2004). Further, while particle fluxes are known to be size dependent (Vong et al., 2010), they are also expected to be chemically dependent (Erisman et al., 1997; Ruijgrok et al., 1997). Models typically include size-dependent particle fluxes, but do not allow for upward fluxes of particles from ecosystem surfaces, let alone chemically-resolved deposition fluxes. Emissions may arise from the release of primary biological particles and the gas-particle conversions in and above vegetation canopies, below the measurement height.

Fluxes of chemical components in the gas or particle phase are driven by turbulent eddies in the atmosphere that operate in the “inertial sub-range”, a range of turbulence typically corresponding to timescales of seconds to minutes. Eddy covariance (EC) uses the covariance between vertical wind speed and species concentration to determine the flux, and is the most commonly used direct method for measuring surface-atmosphere exchange (Baldocchi et al., 1988). EC flux measurements must be taken fast enough to capture the smallest eddies that contribute to the flux – 5 to 10 Hz over

## Eddy covariance HR-AMS aerosol fluxes

D. K. Farmer et al.

Title Page

Abstract

Introduction

Conclusions

References

Tables

Figures



Back

Close

Full Screen / Esc

Printer-friendly Version

Interactive Discussion



most forests. Measurements must be averaged over 30 min, which is long enough to capture the larger flux-relevant eddies, but not so long as to introduce errors from atmospheric non-stationarity. A challenge is making these chemical measurements on a very precise time grid: if data are not collected at evenly spaced intervals, an individual wind speed data point (as measured by a sonic anemometer), for example, may be paired with a concentration data point that was not taken simultaneously, potentially introducing spurious fluxes or smearing out real atmospheric perturbations. Precise data acquisition timing is also required to apply quality assurance controls based on conversions from time to frequency domain (spectral analysis, see Sect. 3.1).

Few instruments are capable of making accurate and precise in situ measurements with enough sensitivity at 10 Hz to determine aerosol fluxes. While frequently applied to CO<sub>2</sub> and other gas phase species, the application of the eddy covariance approach to aerosols has been limited by the stringent instrumental requirements: measurements must not only be portable and free of interference, but they must also be fast and sensitive enough to capture fluctuations on the time scale of flux-carrying turbulent eddies ( $\geq 5$  Hz). Fluxes of total or size-resolved aerosol number (without chemical information) have been performed for some time (e.g., Katen et al., 1985; Sievering, 1987; Buzorius et al., 1998; Dorsey et al., 2002; Martensson et al., 2006; Vong et al., 2010). However, total and chemically-resolved particle mass fluxes have lagged behind because most instruments measuring mass or aerosol chemical composition are far from meeting the rigorous requirements for EC, and most chemically-resolved aerosol flux measurements have been indirect with slower time resolution approaches (e.g., Nemitz et al., 2004b; Trebs et al., 2006; Myles et al., 2007; Thomas et al., 2009; Wolff et al., 2010).

The Aerodyne quadrupole-aerosol mass spectrometer (Q-AMS) was recently adapted to make EC flux measurements of submicron aerosol chemical species (Nemitz et al., 2008). Fluxes by Q-AMS are restricted to about ten mass-to-charge ratios ( $m/z$ ) with unit  $m/z$  resolution, but can include sulphate, nitrate and markers of both hydrocarbon-like organic aerosol (HOA) and oxygenated organic aerosol (OOA) (Nemitz et al., 2008), with the limitation that certain assumptions are needed to derive

**Eddy covariance  
HR-AMS aerosol  
fluxes**

D. K. Farmer et al.

Title Page

Abstract

Introduction

Conclusions

References

Tables

Figures



Back

Close

Full Screen / Esc

Printer-friendly Version

Interactive Discussion



quantitative organic mass fluxes from the monitoring of a few tracer  $m/z$ . Here, we describe the application of a novel, fast data acquisition system (Kimmel et al., 2010) to a high-resolution time-of-flight aerosol mass spectrometer (HR-AMS), which enables direct eddy covariance flux measurements of chemically resolved non-refractory (NR) PM<sub>1</sub> particles with far more chemical information that was possible with the Q-AMS. Making flux measurements at higher mass spectral resolution is necessary for measuring fluxes of a larger array of chemical components, and introduces the potential for measuring ammonium (NH<sub>4</sub><sup>+</sup>) fluxes.

## 2 Methods

### 2.1 Site

We deployed the HR-AMS in alternating eddy covariance/standard modes in a mid-elevation Sierra Nevada ponderosa pine plantation during the BEARPEX-2007 (Biosphere Effects on Aerosols and Photochemistry Experiment) campaign. BEARPEX-2007 took place at the University of California at Berkeley's Blodgett Forest Research Station (1330 m, 38°53.718' N 120°38.041' W) between 10 August and 3 October 2007. The site has been described in detail elsewhere (Goldstein et al., 2000; Murphy et al., 2006; Day et al., 2009). Blodgett Forest is characterized by consistent meteorology in which day-time upslope flows bring air masses influenced by local pine forests, upwind oak forests, and the Greater Sacramento Area in the Central Valley of California (Lamanna et al., 1999; Murphy et al., 2006; Day et al., 2009). Air flows downslope at night, bringing cleaner background air to the site. The site and daytime fetch is located in a plantation dominated by *Pinus ponderosa* L. (ponderosa pine), which was planted in 1990. The understory is composed of *Ceanothus cordulatus* (whitethorn) and *Arcostaphylos* spp. (Manzanita) (Misson et al., 2005). During the BEARPEX-2007 campaign, the canopy had a mean height of 7.9 m; the understory was 2 m. One-sided Leaf Area Index (LAI) for the full canopy was 5.1 m<sup>2</sup> m<sup>-2</sup>. Unless otherwise

## Eddy covariance HR-AMS aerosol fluxes

D. K. Farmer et al.

Title Page

Abstract

Introduction

Conclusions

References

Tables

Figures



Back

Close

Full Screen / Esc

Printer-friendly Version

Interactive Discussion



specified, the measurements presented here represent only a subset of the BEARPEX-2007 project, from 12–27 September 2007, during which both the instrument performance and meteorology were consistent. The inlet and sonic anemometer were 25 m above the ground at the top of a walk-up tower, while the HR-AMS was located in a temperature-controlled container at the bottom of the tower. The HR-AMS inlet was shared with a scanning mobility particle sizer (SMPS), optical particle counter (OPC), and DustTrak; the total flow was controlled by by-pass pumps to be 28.3 Lpm.

## 2.2 Eddy covariance measurements

The mean vertical turbulent flux ( $F_c$ ) crossing the measurement plane over a horizontally homogeneous area (e.g., a forest) is determined as the covariance of vertical wind speed ( $w$ ) and a scalar (such as concentration,  $c$ , of a chemical species) (Baldocchi et al., 1988),

$$F_c = \langle w'c' \rangle \quad (1)$$

The deposition velocity ( $V_{\text{dep}}$ ) is derived from the flux and mean concentration as

$$V_{\text{dep}} = \frac{-F_c}{c} \quad (2)$$

Vertical wind speed was measured with a sonic anemometer (K-style, Applied Technologies, Inc., Longmont, CO, USA). Particles were sampled adjacent (<20 cm) to the sonic anemometer through ~25 m of copper tubing (1.27 cm OD,  $Re \approx 3500$ ) with a wire mesh screen to avoid insect and debris contamination; residence time in the tubing were ~4 s. Chemically resolved particle concentrations (non-refractory  $PM_{10}$ ) were measured with an Aerodyne High-Resolution Time-of-Flight Aerosol Mass Spectrometer (HR-AMS) (DeCarlo et al., 2006; Canagaratna et al., 2007). The HR-AMS focuses particles in the 50–1000 nm size range into a narrow beam with an aerodynamic lens. The beam exits the lens into a vacuum chamber. Particle size is measured by modulating the particle beam with a rotating mechanical chopper and determining

### Eddy covariance HR-AMS aerosol fluxes

D. K. Farmer et al.

Title Page

Abstract

Introduction

Conclusions

References

Tables

Figures

◀

▶

◀

▶

Back

Close

Full Screen / Esc

Printer-friendly Version

Interactive Discussion



**Eddy covariance  
HR-AMS aerosol  
fluxes**

D. K. Farmer et al.

Title Page

Abstract

Introduction

Conclusions

References

Tables

Figures

◀

▶

◀

▶

Back

Close

Full Screen / Esc

Printer-friendly Version

Interactive Discussion



the particle flight time through the chamber, which is a function of the vacuum aerodynamic particle size. At the end of the particle time-of-flight chamber, particles impact a heated surface ( $\sim 600^\circ\text{C}$ ) that flash vaporizes non-refractory species. The resultant vapor plume is ionized by electron ionization (EI, 70 eV), and ions are transferred to a time-of-flight mass spectrometer (HTOF, ToFwerk, Switzerland). The HTOF operates in either a shorter flight path V-mode, or longer W-mode. The V-mode has higher signal, and is thus more sensitive, while the W-mode provides mass spectra with twice the resolution.

The acquisition mode of the HR-AMS was alternated every 30 min between a standard field AMS data acquisition mode (“General Alternation Mode”, see e.g. Canagaratna et al., 2007) and a new flux data acquisition mode (“Flux Mode”). In the General Alternation mode, the HR-AMS was alternated between a 2.5 min average of V-mode mass spectra and particle size-segregated data (PToF) and a 2.5 min average of W-mode mass spectra. The  $m/z$  calibration was performed automatically every 2.5 min during this standard acquisition phase. While in Flux Mode, a novel fast mass spectrometry acquisition system collected particle composition measurements at 5 or 10 Hz. This system is described in detail by Kimmel et al. (2010). Briefly, high-resolution V-mode mass spectra ( $m/z$  range of 11–428) were acquired with a save rate of 10 Hz without particle size modulation. Mass spectra of the transmitted particle and gas beam were acquired continuously for 29 min. This 29 min dataset was preceded and followed (or “bookended”) by 30-second windows of background measurements, in which the particle and gas phase beam was blocked by the mechanical chopper. The difference between the transmitted and averaged background mass spectra was used for flux analysis. The acquisition software forces a time grid based on the computer clock to maintain accurate and precise spacing between the start times of successive measurements. For example, for 10 Hz data collection, the software averaged 92.5 ms of mass spectra, with the remaining 7.5 ms used for transferring the mass spectrum. Note that the measurement was saved even if data could not be both acquired and transferred within the 100 ms window. Saving takes place during the mass spectra averaging for

## Eddy covariance HR-AMS aerosol fluxes

D. K. Farmer et al.

Title Page

Abstract

Introduction

Conclusions

References

Tables

Figures

◀

▶

◀

▶

Back

Close

Full Screen / Esc

Printer-friendly Version

Interactive Discussion



the following datapoint. However, if a measurement could not begin within 0.1 ms of the end of the previous measurement (i.e., transfer took  $>7.5$  ms), it was missed. These missed points were replaced by interpolated values during post-acquisition analysis. Throughout the BEARPEX-2007 field project, this setup typically led to  $<0.5\%$  of the points being missed during a given half-hour, a threshold deemed acceptable for the quality of eddy covariance data. Sonic anemometer data were sent to the HR-AMS computer at 20 Hz via a digital serial port connection. The HR-AMS data acquisition system simultaneously collected wind speed along three axes and temperature on the same time grid as described for mass spectra.

The flux software saved mass spectra at 10 Hz in three formats: (i) complete high-resolution mass spectra, (ii) mass spectra with unit  $m/z$  resolution, and (iii) the total signal within a number of specified high-resolution  $m/z$  ranges. Both unit  $m/z$  resolution (ii) and high-resolution (iii) data are determined as the integrated signal within a defined region of the mass spectrum. The center point of the window for signal summation depends on the ToF- $m/z$  calibration. The number of points integrated into a unit  $m/z$  signal depends on the HTOF resolution, and is always  $\leq m/z$  0.5 of either side of the center (integer) point. For example, the unit  $m/z$  signal for  $m/z$  48 is integrated between  $m/z$  47.879 and  $m/z$  48.193. High resolution  $m/z$  signals are calculated as the sum of signals within a sub-integer range of  $m/z$ , typically corresponding to a consistently isolated mass spectrum peak such as  $\text{NH}_2^+$ . Hereafter, any reference to a unit resolution  $m/z$  signal will be preceded by “UR” (e.g., UR  $m/z$  48 will refer to the unit resolution  $m/z$  48 signal). Any reference to a high-resolution  $m/z$  signal will be preceded by “HR” (e.g., HR  $m/z$  47.9670, or HR  $\text{SO}^+$ ).

Note that for both unit and high-resolution (UR and HR)  $m/z$  signals, the calibration of ion flight time to  $m/z$  is not re-adjusted during the fast flux data collection, but relies on the assumption that the calibration changes negligibly across the 30-min period. Post-acquisition analysis of raw data confirmed that this assumption was met for all BEARPEX-2007 campaign data, but should be re-confirmed for all applications in other environments, particularly where the instrument is subject to temperature fluctuations.

## 2.3 Aerosol flux approaches

Operating the HR-AMS in flux mode allows us to calculate eddy covariance particle fluxes with three different approaches:

- a. Unit  $m/z$  resolution (UR) flux, calculated from unit  $m/z$  signals.
- 5 b. High-resolution (HR) fluxes, calculated from either HR signals that are integrated over a defined window of the mass spectrum (described above), or fitted HR signals, in which the signal for a given ion is calculated from the high-resolution mass spectra by a peak fitting procedure as described elsewhere (e.g., DeCarlo et al., 2006; Müller et al., 2010).
- 10 c. Species fluxes, in which a fragmentation pattern is applied to the mass spectra, sub-dividing UR (or HR) peaks into chemical components before calculating fluxes. This calculation is mathematically identical to the standard AMS data processing that produces, for example, aerosol organic, sulphate, and nitrate concentrations (Allan et al., 2004; Canagaratna et al., 2007).

15 For example, the aerosol sulphate flux could be determined as the flux of (a) UR  $m/z$  48, (b) HR  $\text{SO}^+$  ion (peak centered at  $m/z$  47.9670), or c) a sum of  $\text{H}_x\text{O}_y\text{S}_z^+$  fragments (Canagaratna et al., 2007). In approach (a), the UR flux assumes that sulphate is the only contributing signal to the flux at UR  $m/z$  48. Nemitz et al. (2008) validated this approach for sulphate by comparing flux signals obtained at multiple  $m/z$  thought to  
20 be dominated by sulphate. To avoid confusion, we will hereafter refer to ions observed in the mass spectrometer by their chemical formula (e.g.  $\text{SO}^+$ ,  $\text{NH}_2^+$ ) and chemical species present in aerosol by their complete names (e.g. sulphate, ammonium). Note that all HR fluxes described herein were calculated from HR signals integrated over a defined  $m/z$  range.

## 2.4 Calculations

Particle fluxes are calculated for each of the three approaches (i.e., UR, HR, and species fluxes) with the following protocol:

1. *Time lag correction.* The time lag between the sonic anemometer and HR-AMS is primarily determined by the flow rate through the inlet tubing. For the BEARPEX-2007 inlet configuration, this was approximately 4 s. A more precise determination of time lag can be made with an autocorrelation analysis (Farmer et al., 2006; Nemitz et al., 2008). Time-lag determination through auto-correlation analysis can lead to flux over-estimation in noisy data limited by counting statistics, because it systematically tries to maximize the flux (Taipale et al., 2010). Thus, we used autocorrelation for a sub-set of UR signals throughout the BEARPEX-2007 dataset to find an average time lag for the data. This single determined lagtime of 3.8 s was then applied universally for all measurements described herein.
2. *Sonic anemometer rotation.* To account for the sonic anemometer not being perfectly level with the ground, we also apply a two-dimensional rotation to wind speed in the three axes.
3. *Raw flux calculation.* Raw fluxes and deposition velocities are calculated from the signal by Eqs. (1) and (2). Note that the HR-AMS collects signal in  $(\text{bits} \times \text{ns}) / \text{extraction}$ , and the initial flux is calculated via Eq. (1) in  $(\text{bits} \times \text{ns}) / \text{extraction} \text{ m s}^{-1}$ . This is converted to deposition velocity ( $\text{mm s}^{-1}$ ) via Eq. (2).
4. *WPL correction.* The HR-AMS measures particle mass concentrations, rather than mixing ratios; the Webb-Pearman-Leuning (WPL) correction is thus necessary to account for the changes in air density caused by fluctuations in water vapor (Webb et al., 1980). Corrections for density fluctuations due to temperature are typically ignored for flux measurements with long inlet lines as the tubing is

### Eddy covariance HR-AMS aerosol fluxes

D. K. Farmer et al.

Title Page

Abstract

Introduction

Conclusions

References

Tables

Figures

◀

▶

◀

▶

Back

Close

Full Screen / Esc

Printer-friendly Version

Interactive Discussion



**Eddy covariance  
HR-AMS aerosol  
fluxes**

D. K. Farmer et al.

[Title Page](#)[Abstract](#)[Introduction](#)[Conclusions](#)[References](#)[Tables](#)[Figures](#)[◀](#)[▶](#)[◀](#)[▶](#)[Back](#)[Close](#)[Full Screen / Esc](#)[Printer-friendly Version](#)[Interactive Discussion](#)

expected to dampen temperature fluctuations (Nemitz et al., 2008; Ahlm et al., 2009). For this dataset, the WPL correction is positive (upwards), reducing the total aerosol mass deposition flux by  $\ll 0.1\%$ , with an average correction of  $+0.03\%$ . In recent studies, inlet lines have typically been dried for aerosol composition measurements, which should remove, or at least reduce, the WPL correction. During BEARPEX-2007, we decided not to dry the inlet because of the low ambient humidity at this site; thus, the WPL correction needs to be considered.

5. *Gas-phase corrections.* The HR-AMS measures both the aerosol- and gas-phases, although the former is enriched by a factor of  $\sim 10^7$  compared with the latter. For concentration measurements, the gas-phase contribution is subtracted from the signal by estimating the average contribution from the air beam signal strength derived at  $m/z$  28 ( $N_2^+$ ) and subtracting the signals due to, for example, oxygen and argon ( $O_2^+$ ,  $Ar^+$ ) (Allan et al., 2004). However, this subtraction does not work for short-term fluctuations. Thus, if a gas-phase molecule has a substantial flux, it may contribute to the observed particle flux (Nemitz et al., 2008). Water and  $CO_2$  are the most likely candidates for such interference. As described above for the WPL correction, drying the inlet would remove the water flux interference. During BEARPEX-2007, subtracting the water vapor flux increases the total NR- $PM_1$  flux by less than 1%, a negligible amount. The water vapor flux would affect flux calculations at UR 16, 17, and 18 (i.e., nominal  $m/z$  dominated by  $O^+$ ,  $OH^+$ , and  $H_2O^+$ ). However, as sulphate and organics also contribute to these three UR signals (Allan et al., 2004; Hogrefe et al., 2004), interpreting the particulate water flux would require deconvolution beyond the scope of this study.  $CO_2$  is the other likely gas-phase flux interference.  $CO_2$  dominantly fragments under EI to UR  $m/z$  44 and 28 (Stein, retrieved June 5, 2010) and would thus contribute to the observed organic aerosol flux. This can be corrected by subtracting the observed gas-phase  $CO_2$  flux, which is commonly measured during field projects, from the UR  $m/z$  44 flux signal (or the HR  $CO_2^+$  fragment) taking into account the efficiency with which the HR-AMS detects gas-phase  $CO_2$ ,

relative to aerosol-derived  $\text{CO}_2^+$  ( $1.9 \times 10^{-7}$  during this campaign). The largest gas-phase  $\text{CO}_2$  flux observed during BEARPEX-2007,  $-58 \mu\text{mol m}^{-2} \text{h}^{-1}$ , would thus be observed by the HR-AMS as a flux of  $-0.07 \text{ ng m}^{-2} \text{ s}^{-1}$ . The gas-phase  $\text{CO}_2$  correction is, on average,  $-0.4\%$  for the aerosol flux at UR  $m/z$  44, a negligible correction for the total NR- $\text{PM}_1$  mass flux. While the correction ranges between  $-98$  and  $+55\%$ , the extremes occur rarely, and only when the observed UR  $m/z$  44 flux is near zero and below its detection limit.

6. *Corrected flux calculation.* The deposition velocities can be reconverted to flux in more typical units of  $\mu\text{g m}^{-2} \text{ s}^{-1}$  by multiplying by average mass concentrations derived from the standard HR-AMS analysis for either the flux period, or the average from the data collected before and after the half-hour flux measurements. This is mathematically identical to converting every 10 Hz datapoint into a mass concentration from a raw signal and calculating the flux using the mass concentration time series (Nemitz et al., 2008).

### 3 Constraints on particle fluxes by HR-AMS

To quantify the ability of the HR-AMS to measure chemically-resolved aerosol fluxes, we use three approaches: (i) Spectral analysis to demonstrate that the HR-AMS meets the instrumental requirements for eddy covariance flux measurements (Sect. 3.1); (ii) Quantitative constraints on uncertainty for both individual flux measurements and the entire dataset (Sect. 3.2); and (iii) Internal comparisons (Sect. 3.3) to demonstrate that HR-AMS UMR and HR fragment fluxes accurately describe the fluxes of given aerosol chemical components.

## Eddy covariance HR-AMS aerosol fluxes

D. K. Farmer et al.

Title Page

Abstract

Introduction

Conclusions

References

Tables

Figures

⏪

⏩

◀

▶

Back

Close

Full Screen / Esc

Printer-friendly Version

Interactive Discussion



### 3.1 Instrument time response

As described above, instruments used for eddy covariance flux measurements must be both fast and sensitive. Further, concentration measurements must not vary within the time-scale of the analysis, the stationarity requirement (Kaimal et al., 1994). Figure 1 shows that the fast time resolution (10 Hz) HR-AMS particle signal is clearly distinguishable over instrument background, evidenced by comparing the background (first and last 30 s for a given flux period) and transmitted (continuous 29 min) time periods. Composition changes are clearly visible, though rarely occurred over rapid timescales within the 30-min flux measurement periods during the BEARPEX-2007 campaign due to the site's remoteness and consistent meteorology, thus typically meeting eddy covariance requirements for stationarity. Further, individual high resolution mass spectra show clear peaks above the noise (Fig. 2). However, the observation of mass spectral signal above the noise does not demonstrate that the HR-AMS measurements are sensitive enough to measure fluxes over forests. An additional diagnostic tool for EC measurements is spectral analysis.

Figure 3 shows a typical frequency-multiplied co-spectrum obtained from the covariance between the vertical velocity ( $w$ ) and the HR-AMS signal for a single flux measurement – in this case, the HR  $\text{NH}_2^+$  fragment taken between 04:00–04:30 p.m., 7 September 2007. Both the frequency-binned average and the entire set of 10 Hz observations are included. The frequency-binned data exhibit a (frequency) $^{-4/3}$  response between 0.005 and 2.5 Hz. This frequency response is characteristic of the inertial sub-range as predicted from dimensional analysis through the Kolmogorov theory (Kaimal et al., 1994). The inertial sub-range is an intermediate range of turbulent scales characterized by energetic equilibrium; measurements should encompass this sub-range of turbulence for accurate eddy covariance fluxes. Deviations from this frequency response trend towards a steeper slope at higher frequencies would be evidence of “spectral attenuation”, or underestimation of fluxes due to either damping of high-frequency signals within the sampling lines or slow instrument response. Such

## Eddy covariance HR-AMS aerosol fluxes

D. K. Farmer et al.

Title Page

Abstract

Introduction

Conclusions

References

Tables

Figures



Back

Close

Full Screen / Esc

Printer-friendly Version

Interactive Discussion



deviations are not observed in Fig. 3, nor in most daytime BEARPEX-2007 HR-AMS co-spectra, indicating that the turbulent inlet flow minimized attenuation and that the instrument response is sufficiently fast.

Co-spectra are often used in eddy covariance analysis to determine whether flux measurements were averaged over long enough periods of time to capture all flux-carrying eddies. Figure 3 shows that the low-frequency eddies ( $<0.004$  Hz, corresponding to a spatial scale  $>750$  m for a wind speed of  $3 \text{ m s}^{-1}$ ) may still contribute some flux signal and that averaging for longer than 29 min may cause a slight increase in the flux. However, as described in Nemitz et al. (2008) for similar Q-AMS co-spectra, this slight increase in flux would be captured at the expense of longer averaging times and a potential lack of stationarity.

### 3.2 Detection limits and uncertainty

Several sources contribute to the uncertainty of a single flux measurement. Instrument noise causes random errors. Attenuation from air flow smearing in the sample tubing and the distance between the aerosol inlet and sonic anemometer can cause underestimates of flux, and are thus systematic errors. However, as described by Nemitz et al. (2008), because a small number of particles are sampled during a 100 ms measurement period, particle flux measurements are typically limited by particle counting statistics. Further, particle size affects the flux measurement, as larger particles are fewer in number, but carry the majority of the total particle mass: Jimenez et al. (2003) reported that 2% of the particle number represented 50% of the submicron particle mass for an ambient dataset in Massachusetts, USA. Such large particles appear as spikes in a fast time series (e.g., Fig. 1). As they contribute real flux, these large particles generally should not be removed by the de-spiking routines commonly used for gas-phase flux measurements (Nemitz et al., 2008).

Nemitz et al. (2008) proposed using the fact that a single chemical component (e.g. sulphate) can be observed in two different  $m/z$  ratios as an alternative method to estimate flux errors (Fig. 4). The typical error for a given species can thus be calculated

## Eddy covariance HR-AMS aerosol fluxes

D. K. Farmer et al.

Title Page

Abstract

Introduction

Conclusions

References

Tables

Figures



Back

Close

Full Screen / Esc

Printer-friendly Version

Interactive Discussion



## Eddy covariance HR-AMS aerosol fluxes

D. K. Farmer et al.

Title Page

Abstract

Introduction

Conclusions

References

Tables

Figures

⏪

⏩

◀

▶

Back

Close

Full Screen / Esc

Printer-friendly Version

Interactive Discussion

from the standard deviation of flux differences between the two UR  $m/z$  ratios. Thus for sulphate, the  $1\sigma$  error is  $0.117 \text{ ng m}^{-2} \text{ s}^{-1}$ , corresponding to a  $3\sigma$  DL for sulphate fluxes of  $\pm 0.35 \text{ ng m}^{-2} \text{ s}^{-1}$ . While this is significantly less than the  $\pm 6.2 \text{ ng m}^{-2} \text{ s}^{-1}$  DL reported for the Q-AMS sulphate fluxes over Boulder (Nemitz et al., 2008), the magnitude of the observed sulphate fluxes was much smaller during BEARPEX-2007 than at Boulder, and the ratio of DL to average observed flux is within the same order of magnitude for the two projects. We calculate a BEARPEX-2007 nitrate flux DL from UR  $m/z$  30 and 46 of  $\pm 0.095 \text{ ng m}^{-2} \text{ s}^{-1}$ . It should be noted, however, that for the Q-AMS system this error includes the particle counting error: for each particle arrival, the quadrupole MS detects only signal at a single UM  $m/z$ , fluxes of the same component derived from different  $m/z$  represents different particle populations. In contrast, the HR-AMS measures all  $m/z$  simultaneously, and the two fluxes reflect the same particle population. Thus, for this instrument, the comparison between the two sulphate fluxes does not provide information on the uncertainties due to particle counting statistics. This explains the lower DL of the HR-AMS, and indicates that, for the new instrument, this approach to error analysis does not capture the full uncertainty, and a different approach needs to be followed.

As described in Wienhold et al. (1995), the uncertainty of a single flux measurement can be derived from the baseline fluctuation in the cross correlation function between vertical wind speed and the scalar of interest, calculated with lag times significantly longer than the delay time. This provides an alternative empirical measurement of the detection limit, which should represent a more comprehensive definition of uncertainty. We calculated the precision, and thus detection limit (DL), of a single flux measurement to be  $3 \times \sigma_{F,\text{lag}}$ , where  $\sigma_{F,\text{lag}}$  is the standard deviation of the fluxes calculated with lag-times offset by between 50 and 80 s. For example, this metric provided a relative error ( $1\sigma$ ) of the high resolution  $\text{NH}_2^+$  fragment of 60%, or  $0.49 \text{ ng m}^{-2} \text{ s}^{-1}$ , for the single flux measurement taken between 04:00–04:30 p.m., 7 September 2007. The median  $1\sigma$  relative error for the complete ensemble of HR  $\text{NH}_3^+$  fluxes from BEARPEX-2007 was 62% (mode 20%, mean 248%), corresponding to a median DL of  $\pm 0.42 \text{ ng m}^{-2} \text{ s}^{-1}$ .



Relative errors for BEARPEX-2007 HR  $\text{NH}_2^+$  fluxes were similar (median 65%, mode 35%, mean 360%), corresponding to median DL of  $\pm 0.43 \text{ ng m}^{-2} \text{ s}^{-1}$ . Thus, during this campaign, the typical single half-hour flux measurement for the ammonium fragments was below the detection limit, and averages of multiple points must be used for scientific interpretation.

In contrast, fluxes of UR  $m/z$  fluxes dominated by nitrate or sulphate such as UR  $m/z$  46 (mostly  $\text{NO}_2^+$  from nitrate) and UR  $m/z$  64 (mostly  $\text{SO}_2^+$  from sulphate) have much smaller relative errors and lower detection limits. For example, the relative error for a single flux measurement at UR  $m/z$  46 (12:00–12:30, 15 September 2007) is 18%, corresponding to a  $3\sigma$  detection limit for an individual 30-min nitrate flux measurement via the UR 46 signal of  $\pm 0.56 \text{ ng m}^{-2} \text{ s}^{-1}$ , below the observed flux of  $-1.04 \text{ ng m}^{-2} \text{ s}^{-1}$ . Sulphate fluxes derived from UR  $m/z$  64 during the BEARPEX-2007 campaign had median  $1\sigma$  relative errors of 60% (20% mode, 194% mean). However, the DL for UR 64 fluctuated between  $0.05\text{--}6.4 \text{ ng m}^{-2} \text{ s}^{-1}$ , with a median value of  $1.15 \text{ ng m}^{-2} \text{ s}^{-1}$  (mode 0.4, mean  $1.49 \text{ ng m}^{-2} \text{ s}^{-1}$ ). The particle flux errors as derived by this lagged covariance approach increase with the magnitude of the flux, although they do not result in a constant relative error. Flux errors increase with wind speed and friction velocity, and the rate of increase is greater at higher wind speeds ( $>2 \text{ m s}^{-1}$ ). The behavior of the particle flux errors suggests that larger wind speeds, which increase mixing between the forest canopy and atmosphere, increase particle emission and deposition and its associated uncertainty. Similarly, the DL is larger during the daytime than nighttime for UR  $m/z$  64. These findings are consistent with theoretical considerations that show that during windier/more turbulent conditions, a concentration measurement needs to be more precise to resolve the same flux. For example, Fairall (1984) showed that the error in  $V_d$  increases with increasing standard deviation in vertical wind speed ( $\sigma_w$ ). Rowe et al. (2010) demonstrated that sensor resolution requirements increase with increasing  $u_*$  and for unstable conditions. The error considered here is the error in determining the correct local co-variance between  $c$  and  $w$ . Additional error is introduced in that the local flux detected during a 29-min period

**Eddy covariance  
HR-AMS aerosol  
fluxes**

D. K. Farmer et al.

Title Page

Abstract

Introduction

Conclusions

References

Tables

Figures

◀

▶

◀

▶

Back

Close

Full Screen / Esc

Printer-friendly Version

Interactive Discussion



at a single position may not be statistically representative of the average flux over the surface. Even two “perfect” eddy-covariance flux measurement systems would therefore not derive the same flux and this error decreases with increasing turbulence (e.g., Hollinger et al., 2005; Nemitz et al., 2009b, and references therein).

### 3.3 Internal comparisons and validation

We use internal comparisons to determine whether UR  $m/z$  particle fluxes are appropriate proxies for a species flux. UR  $m/z$  particle fluxes have the advantage over species fluxes of being less computationally expensive. Thus, we compare UR  $m/z$  particle fluxes for  $m/z$  dominated by nitrate, sulphate, or organic ions. For example, in terms of the concentration measurements, UR  $m/z$  48 is dominated by  $\text{SO}_4^+$ , while UR  $m/z$  64 is dominated by  $\text{SO}_2^+$ . To determine whether the flux at these two nominal masses can be used as a proxy for the sulphate flux, we compare the UR  $m/z$  signals, fluxes and deposition velocities (Fig. 4a–c). Because there are errors associated with values for both  $m/z$ 's, the linear regression analysis uses a robust regression based on absolute deviations on both coordinates. For mass concentrations, we use the standard deviation of observed mass concentrations within a given half-hour measurement period as weights for each datapoint in the regression. For the fluxes, we calculated uncertainties for a single measurement with the lagged covariance approach (Sect. 3.2). Uncertainties for individual deposition velocity measurements were calculated following error propagation from the flux and concentration uncertainties. The signals are linearly correlated with a slope depending on the fragmentation of sulphate in the AMS; Fig. 4a shows that ambient sulphate fragments to  $\text{SO}_2^+$  in a slightly larger fraction than to  $\text{SO}_4^+$ . Similarly, the two UR fluxes are linearly correlated, with a slope representative of the different contributions to the fluxes of the two fragments (Fig. 4b). Note that removing the two outlying points improves the correlation ( $r^2=0.80$ ), but does not change the slope or intercept. This correlation is consistent with the signals at UR  $m/z$  48 and 64 being controlled by the same mechanisms, providing evidence that both UR  $m/z$  signals are dominated by sulphate. While the magnitude of both the signals and fluxes

## Eddy covariance HR-AMS aerosol fluxes

D. K. Farmer et al.

Title Page

Abstract

Introduction

Conclusions

References

Tables

Figures

◀

▶

◀

▶

Back

Close

Full Screen / Esc

Printer-friendly Version

Interactive Discussion



are not necessarily the same due to fragmentation patterns, the deposition velocity (Fig. 4c) should represent the overall sulphate deposition. In the absence of additional peaks in high resolution data indicating potential interferences, a non-unity slope can be interpreted as the uncertainty in sulphate deposition velocity. Thus, the slope of 0.90 suggests that the mean deposition velocity calculated from a single sulphate fragment has an uncertainty of  $\sim 10\%$ .

Unlike the sulphate-derived  $\text{SO}^+$  and  $\text{SO}_2^+$  signals at UR  $m/z$  48 and 64, which generally only have much smaller contributions from organic species, particulate ammonium dominantly fragments to  $\text{NH}^+$ ,  $\text{NH}_2^+$  and  $\text{NH}_3^+$ , which overlap in the UR mass spectrum with  $\text{CH}_3^+$ ,  $\text{O}^+$  and  $\text{OH}^+$  at  $m/z$  15, 16 and 17, respectively (e.g. inset, Fig. 2). The  $\text{O}^+$  and  $\text{OH}^+$  fragments are typically much larger than the ammonium fragments in the mass spectrometer background (due to residual  $\text{H}_2\text{O}$ ); both particulate and gas-phase  $\text{H}_2\text{O}$  also contribute to the transmitted signal. The  $\text{CH}_3^+$  aerosol fragment is of similar magnitude to  $\text{NH}^+$ . Thus quantification of ammonium fluxes at unit mass resolution is particularly difficult. In standard UR AMS concentration data, this is typically dealt with by use of the fragmentation table (Allan et al., 2004), and accepting a higher level of noise for ammonium than other species (e.g., DeCarlo et al., 2006). However, because fluxes can have both negative and positive components, and can change in both magnitude and direction throughout the day, creation of a separate, robust fragmentation table for fluxes is difficult. While the calculation of “species fluxes” through application of the standard fragmentation table to every 0.1 s measurement point is as valid as its application to routine HR-AMS data analysis, it is not only computationally expensive, but also can result in large uncertainties where a flux is calculated from a UR  $m/z$  that is subject to a large gas-phase correction: small absolute random noise in the air beam signal will induce large relative noise for the aerosol mass derived from these peaks. In contrast, the increased resolution of the HR-AMS allows for the mass spectral separation of these interferences and creates the potential to measure particulate ammonium fluxes. Figure 4d–f shows the correlation in signal, flux and deposition velocity for HR  $\text{NH}_2^+$  and  $\text{NH}_3^+$  ions, integrated between  $m/z$  16.010–16.040

**Eddy covariance  
HR-AMS aerosol  
fluxes**

D. K. Farmer et al.

Title Page

Abstract

Introduction

Conclusions

References

Tables

Figures

◀

▶

◀

▶

Back

Close

Full Screen / Esc

Printer-friendly Version

Interactive Discussion





dominated by biogenic emissions and less influenced by the agricultural or combustion sources that tend to play a larger role later in the day (Lamanna et al., 1999; Day et al., 2009).

A detailed presentation and analysis of particle fluxes is beyond the scope of this manuscript, but diurnal observations for both total aerosol and ammonium from HR  $\text{NH}_2^+$  are presented in Figs. 6 and 7, respectively. On average, deposition of both total  $\text{NR-PM}_1$  and submicron ammonium were observed, with maximum deposition velocities occurring in the late morning. Note that total  $\text{NR-PM}_1$  fluxes were calculated as the sum of species fluxes. Deposition velocities for a given subset of data are derived from the negative slope of flux as a function of mass concentration. From the slope of flux versus mass concentration for noon-time data, the magnitude of the  $\text{NH}_2^+$  fragment deposition ( $1.9 \pm 0.7 \text{ mm s}^{-1}$ ) is within the uncertainty of total  $\text{PM}_1$  deposition velocities ( $2.05 \pm 0.04 \text{ mm s}^{-1}$ ).

## 5 Discussion

### 5.1 HR-AMS eddy covariance fluxes

In this manuscript, we presented three approaches to defining fluxes: UR  $m/z$ , HR and species fluxes. Each of these approaches makes assumptions. The UR  $m/z$  flux gives a combined flux signal comprised of individual contributions from each ion present at the mass, which may have fluxes of different magnitudes and signs. The contribution of different ions to the flux of a given UR  $m/z$  is not necessarily equivalent to the contribution of those ions to the signal, or mass, at that  $m/z$ . Comparing fluxes and concentrations for two UR  $m/z$  attributed to the same chemical component provides validation of this approach. HR fluxes rely on the integration of data points within a defined  $m/z$  window, and require either that fragments are isolated from a parent peak, as is the case for  $\text{NH}_2^+$  (inset, Fig. 2), or that the peak can be clearly distinguished in fast mass spectra by use of a fitting routine. Species fluxes share the same set of

## Eddy covariance HR-AMS aerosol fluxes

D. K. Farmer et al.

Title Page

Abstract

Introduction

Conclusions

References

Tables

Figures

◀

▶

◀

▶

Back

Close

Full Screen / Esc

Printer-friendly Version

Interactive Discussion



**Eddy covariance  
HR-AMS aerosol  
fluxes**

D. K. Farmer et al.

Title Page

Abstract

Introduction

Conclusions

References

Tables

Figures

◀

▶

◀

▶

Back

Close

Full Screen / Esc

Printer-friendly Version

Interactive Discussion



caveats as mass concentrations (Canagaratna et al., 2007), along with the additional uncertainties of correcting for gas-phase contributions. Validation of the fluxes using correlations of fluxes calculated from several ions or  $m/z$  as described here (Fig. 4) provides additional insight on interpreting fluxes, and is highly recommended for future studies.

It is important to realize that HR-AMS fluxes are subject to the same interpretation uncertainties as standard AMS mass concentrations calculated by well-established routines (e.g., Canagaratna et al., 2007). In particular, the sulphate, nitrate and ammonium fluxes are not necessarily due to pure inorganic components. Organic sulphates are known to fragment to inorganic  $H_xSO_y^+$  ions indistinguishably from inorganic ammonium sulphate (Farmer et al., 2010). Organic nitrates fragment to  $NO_x^+$  ions slightly differently from ammonium nitrate, but not so differently as to enable easy quantification given variations in the organic nitrate fragmentation and potential contributions from mineral nitrates and possibly nitrites. Thus HR-AMS derived sulphate and nitrate fluxes must be considered the sum of both organic and inorganic components (Farmer et al., 2010). The  $CH_3SO_2^+$  HR fragment may help to separate organic sulphate and organic sulfonic acid contributions from inorganic sulphate. Additionally, amines and other reduced organic nitrogen components of aerosol may produce  $NH_2^+$  and  $NH_3^+$  fragments (Sun et al., 2010) that may contribute to the observed particulate ammonium fluxes derived from HR fragments.

Further, in interpreting these HR-AMS fluxes, it is important to realize that aerosol chemical components (e.g. nitrate) may be affected by chemistry and changes in the gas/aerosol partitioning (e.g., photochemistry, uptake on aerosol surfaces, evaporation to or condensation from the gas phase). As a result, the flux observed at the measurement height will not only represent the surface flux, but will also include any chemical sources and sinks below the measurement height. In addition, the fluxes are derived from the aerosol mass within a certain size-range, which may not be a conserved parameter where the aerosol size changes beyond the upper or lower size cut-off during vertical transport. By integrating over the total accumulation mode mass

**Eddy covariance  
HR-AMS aerosol  
fluxes**

D. K. Farmer et al.

[Title Page](#)[Abstract](#)[Introduction](#)[Conclusions](#)[References](#)[Tables](#)[Figures](#)[⏪](#)[⏩](#)[◀](#)[▶](#)[Back](#)[Close](#)[Full Screen / Esc](#)[Printer-friendly Version](#)[Interactive Discussion](#)

of the chemical components, the HR-AMS is relatively insensitive to changes in size distribution within the instrument's submicron range, and we can generally consider the HR-AMS flux measurement to be insensitive to artifacts due to the small changes in submicron particle size caused by evaporation/condensational growth, which have been found to affect the measurement of size-segregated particle number fluxes within individual accumulation mode size bins or fluxes of total particle number above a specified cutoff (e.g., Nemitz et al., 2004a, 2009a; Vong et al., 2010). Under some conditions, however, vertical gradients in particle growth in or out of the AMS-observable size range due to water uptake or changes in gas/aerosol partitioning with condensable chemical species could, however, cause an artifact. More detailed analyses are required to parse out such effects on surface flux measurements, and will be pursued in future manuscripts.

## 5.2 BEARPEX-2007

We observed deposition of NR-PM<sub>1</sub> during the BEARPEX-2007 campaign, consistent with particle number fluxes (Vong et al., 2010). Ammonium deposited to the forest surface. To our knowledge, the measurements described here include the first direct eddy covariance flux measurements of particulate ammonium. Availability of instrumentation has limited past studies to indirect flux methods (Nemitz et al., 2004b; Trebs et al., 2006; Wolff et al., 2010). Ammonium is an unusually challenging aerosol component for which to interpret fluxes, as one subset of ammonium is irreversibly tied to sulphate ions, while another is in equilibrium with gas-phase species:



The flux of any single species in R1 may be subject to chemical flux divergence through the canopy. HR-AMS ammonium deposition velocities for BEARPEX-2007 are consistent with previous measurements at other sites (Nemitz et al., 2004b), but an order of magnitude less than the total NH<sub>3(g)</sub>+particulate ammonium deposition velocities observed over a spruce forest in Germany (Wolff et al., 2010). To understand the

observed ammonium fluxes and mass concentrations, we use the observed balance between NR-PM<sub>1</sub> cations and anions, also known as the “ammonium balance”. This is the comparison between ammonium observed (the positively charged component, or cations) and ammonium concentration required to balance the charges of the observed particulate sulphate, nitrate and chloride (the negatively charged component, or anions). During the BEARPEX-2007 project, we observed ammonium concentrations that were, within the uncertainties, equivalent to the calculated amount needed to neutralize the observed anions (Fig. 8a, robust regression slope = 0.94,  $r^2 = 0.92$ ). Except for a few isolated time periods when nitrate was elevated, sulphate dominated the total anion charge. Ammonium sulphate is effectively non-volatile, and would not be subject to flux divergence driven by evaporation, while its production is limited by local H<sub>2</sub>SO<sub>4</sub> production. Further, due to the small contribution of ammonium nitrate to PM<sub>1</sub> mass during BEARPEX-2007, it is unlikely that NH<sub>4</sub>NO<sub>3</sub> evaporation would have been significant, and NH<sub>3(g)</sub> concentrations are too low at this site to support NH<sub>4</sub>NO<sub>3</sub> production (<1–2 ppb) (Fischer et al., 2007). Similar to the concentrations, the cation flux (observed ammonium) was well correlated with the anion flux (Fig. 8b, robust regression slope = 0.94, intercept =  $-0.05 \text{ neq m}^{-2} \text{ s}^{-1}$ ,  $r^2 = 0.46$ ). On average, sulphate and nitrate fluxes balanced 2/3 and 1/3 of the ammonium fluxes, respectively. Ammonium chloride is a minor component at Blodgett, and chloride fluxes typically contributed <2% of the anion charge flux.

The HR-AMS ammonium deposition velocities can be compared to particle deposition models. Ruijgrok et al. (1997) used data collected over the Dutch Speulder Bos experimental forest to propose a chemically-resolved deposition parameterization that depends on friction velocity and relative humidity. However, the Ruijgrok parameterization provides a substantial (~40%) overestimate of ammonium fluxes during BEARPEX-2007. This would be consistent with the measurements used by Ruijgrok et al. (1997) being enhanced by NH<sub>4</sub>NO<sub>3</sub> volatilization during deposition. Ammonium at Speulder Bos was dominantly bound to nitrate, as opposed to sulphate during BEARPEX-2007.

**Eddy covariance  
HR-AMS aerosol  
fluxes**

D. K. Farmer et al.

Title Page

Abstract

Introduction

Conclusions

References

Tables

Figures

◀

▶

◀

▶

Back

Close

Full Screen / Esc

Printer-friendly Version

Interactive Discussion



## 6 Conclusions

We have presented a new system for measuring chemically-resolved aerosol fluxes using the HR-AMS. We have demonstrated that the HR-AMS can be used with the eddy covariance acquisition software alongside a sonic anemometer to measure chemically resolved particle fluxes. Such chemically-resolved mass fluxes have the potential to provide different information from particle number fluxes. Differences in flux between chemically resolved components have the potential to provide additional information relevant to regional air quality and global atmospheric chemistry models. Further, we demonstrate the first direct observations of particulate ammonium deposition over a forest. The anion/cation balance in both concentrations and fluxes show that the ammonium flux during BEARPEX-2007 is dominated by ammonium sulphate.

The approach described here for HR-AMS fluxes could be applied to other TOF mass spectrometers, including chemical ionization TOFMS instruments for more accurate and precise flux measurements of VOCs and other trace gases than are typically available with the more widely used quadrupole mass spectrometer flux measurements.

*Acknowledgement.* We thank Alex Guenther and Andrew Turnipseed from NCAR for lending us a sonic anemometer for the BEARPEX-2007 study. We also thank BFRS staff for their logistical support and Sierra Pacific Industries for providing access to their property. This work was partially supported by NSF ATM-0449815 and ATM-0919189, and by NASA NNX08AD39G and by the UK Natural Environment Research Council through the DIASPORA grant (NE/E007309/1). D. Farmer acknowledges a NOAA Climate and Global Change Postdoctoral Fellowship.

## Eddy covariance HR-AMS aerosol fluxes

D. K. Farmer et al.

Title Page

Abstract

Introduction

Conclusions

References

Tables

Figures

◀

▶

◀

▶

Back

Close

Full Screen / Esc

Printer-friendly Version

Interactive Discussion



## References

- Ahlm, L., Nilsson, E. D., Krejci, R., Mårtensson, E. M., Vogt, M., and Artaxo, P.: Aerosol number fluxes over the Amazon rain forest during the wet season, *Atmos. Chem. Phys.*, 9, 9381–9400, doi:10.5194/acp-9-9381-2009, 2009.
- 5 Allan, J. D., Delia, A. E., Coe, H., Bower, K. N., Alfarra, M. R., Jimenez, J. L., Middlebrook, A. M., Drewnick, F., Onasch, T. B., Canagaratna, M. R., Jayne, J. T., and Worsnop, D. R.: A generalised method for the extraction of chemically resolved mass spectra from aerodyne aerosol mass spectrometer data, *J. Aerosol Sci.*, 35, 909–922, 2004.
- 10 Baldocchi, D. D., Hicks, B. B., and Meyers, T. P.: Measuring biosphere-atmosphere exchanges of biologically related gases with micrometeorological methods, *Ecology*, 69, 1331–1340, 1988.
- Bessagnet, B., Seigneur, C., and Menut, L.: Impact of dry deposition of semi-volatile organic compounds on secondary organic aerosols, *Atmos. Environ.*, 44, 1781–1787, 2010.
- 15 Brook, R. D., Rajagopalan, S., Pope, C. A., Brook, J. R., Bhatnagar, A., Diez-Roux, A. V., Holguin, F., Hong, Y. L., Luepker, R. V., Mittleman, M. A., Peters, A., Siscovick, D., Smith, S. C., Whitsel, L., and Kaufman, J. D.: Particulate matter air pollution and cardiovascular disease: an update to the scientific statement from the American Heart Association, *Circulation*, 121, 2331–2378, 2010.
- 20 Buzorius, G., Rannik, U., Makela, J. M., Vesala, T., and Kulmala, M.: Vertical aerosol particle fluxes measured by eddy covariance technique using condensational particle counter, *J. Aerosol Sci.*, 29, 157–171, 1998.
- Canagaratna, M. R., Jayne, J. T., Jimenez, J. L., Allan, J. D., Alfarra, M. R., Zhang, Q., Onasch, T. B., Drewnick, F., Coe, H., Middlebrook, A., Delia, A., Williams, L. R., Trimborn, A. M., Northway, M. J., DeCarlo, P. F., Kolb, C. E., Davidovits, P., and Worsnop, D. R.: Chemical and microphysical characterization of ambient aerosols with the Aerodyne aerosol mass spectrometer, *Mass Spectrom. Rev.*, 26, 185–222, 2007.
- 25 Day, D. A., Farmer, D. K., Goldstein, A. H., Wooldridge, P. J., Minejima, C., and Cohen, R. C.: Observations of  $\text{NO}_x$ ,  $\Sigma\text{PNs}$ ,  $\Sigma\text{ANs}$ , and  $\text{HNO}_3$  at a Rural Site in the California Sierra Nevada Mountains: summertime diurnal cycles, *Atmos. Chem. Phys.*, 9, 4879–4896, doi:10.5194/acp-9-4879-2009, 2009.
- 30

AMTD

3, 5867–5905, 2010

### Eddy covariance HR-AMS aerosol fluxes

D. K. Farmer et al.

Title Page

Abstract

Introduction

Conclusions

References

Tables

Figures

◀

▶

◀

▶

Back

Close

Full Screen / Esc

Printer-friendly Version

Interactive Discussion



**Eddy covariance  
HR-AMS aerosol  
fluxes**

D. K. Farmer et al.

[Title Page](#)[Abstract](#)[Introduction](#)[Conclusions](#)[References](#)[Tables](#)[Figures](#)[◀](#)[▶](#)[◀](#)[▶](#)[Back](#)[Close](#)[Full Screen / Esc](#)[Printer-friendly Version](#)[Interactive Discussion](#)

DeCarlo, P. F., Kimmel, J. R., Trimborn, A., Northway, M. J., Jayne, J. T., Aiken, A. C., Gonin, M., Fuhrer, K., Horvath, T., Docherty, K. S., Worsnop, D. R., and Jimenez, J. L.: Field-deployable, high-resolution, time-of-flight aerosol mass spectrometer, *Anal. Chem.*, 78, 8281–8289, 2006.

5 Dominici, F., Peng, R. D., Bell, M. L., Pham, L., McDermott, A., Zeger, S. L., and Samet, J. M.: Fine particulate air pollution and hospital admission for cardiovascular and respiratory diseases, *JAMA-J. Am. Med. Assoc.*, 295, 1127–1134, 2006.

Dorsey, J. R., Nemitz, E., Gallagher, M. W., Fowler, D., Williams, P. I., Bower, K. N., and Beswick, K. M.: Direct measurements and parameterisation of aerosol flux, concentration and emission velocity above a city, *Atmos. Environ.*, 36, 791–800, 2002.

10 Erisman, J. W., Draaijers, G., Duyzer, J., Hofschreuder, P., VanLeeuwen, N., Romer, F., Ruijgrok, W., Wyers, P., and Gallagher, M.: Particle deposition to forests – summary of results and application, *Atmos. Environ.*, 31, 321–332, 1997.

Fairall, C. W.: Interpretation of eddy-correlation measurements of particulate deposition and aerosol flux, *Atmos. Environ.*, 18, 1329–1337, 1984.

15 Farmer, D. K., Wooldridge, P. J., and Cohen, R. C.: Application of thermal-dissociation laser induced fluorescence (TD-LIF) to measurement of  $\text{HNO}_3$ ,  $\Sigma$ alkyl nitrates,  $\Sigma$ peroxy nitrates, and  $\text{NO}_2$  fluxes using eddy covariance, *Atmos. Chem. Phys.*, 6, 3471–3486, doi:10.5194/acp-6-3471-2006, 2006.

20 Farmer, D. K., Matsunaga, A., Docherty, K., Surratt, J. D., Seinfeld, J. H., Ziemann, P. J., and Jimenez, J. L.: Response of an aerosol mass spectrometer to organonitrates and organosulfates and implications for atmospheric chemistry, *P. Natl. Acad. Sci. USA*, 107, 6670–6675, 2010.

25 Fischer, M. L. and Littlejohn, D.: Measurements of ammonia at Blodgett Forest, prepared for State of California Air Resources Board, Lawrence Berkeley National Laboratory, Berkeley, 2007.

Goldstein, A. H., Hultman, N. E., Fracheboud, J. M., Bauer, M. R., Panek, J. A., Xu, M., Qi, Y., Guenther, A. B., and Baugh, W.: Effects of climate variability on the carbon dioxide, water, and sensible heat fluxes above a ponderosa pine plantation in the Sierra Nevada (CA), *Agr. Forest Meteorol.*, 101, 113–129, 2000.

30 Hogrefe, O., Drewnick, F., Lala, G. G., Schwab, J. J., and Demerjian, K. L.: Development, operation and applications of an aerosol generation, calibration and research facility, *Aerosol Sci. Technol.*, 38, 196–214, 2004.

**Eddy covariance  
HR-AMS aerosol  
fluxes**

D. K. Farmer et al.

[Title Page](#)[Abstract](#)[Introduction](#)[Conclusions](#)[References](#)[Tables](#)[Figures](#)[◀](#)[▶](#)[◀](#)[▶](#)[Back](#)[Close](#)[Full Screen / Esc](#)[Printer-friendly Version](#)[Interactive Discussion](#)

- Hollinger, D. Y. and Richardson, A. D.: Uncertainty in eddy covariance measurements and its application to physiological models, *Tree Physiol.*, 25, 873–885, 2005.
- Isaksen, I. S. A., Granier, C., Myhre, G., Berntsen, T. K., Dalsøren, S. B., Gauss, M., Klimont, Z., Benestad, R., Bousquet, P., Collins, W., Cox, T., Eyring, V., Fowler, D., Fuzzi, S., Jöckel, P., Laj, P., Lohmann, U., Maione, M., Monks, P., Prevot, A. S. H., Raes, F., Richter, A., Rognerud, B., Schulz, M., Shindell, D., Stevenson, D. S., Storelvmo, T., Wang, W.-C., van Weele, M., Wild, M., and Wuebbles, D.: Atmospheric composition change: climate-chemistry interactions, *Atmos. Environ.*, 43, 5138–5192, 2009.
- Jimenez, J. L., Jayne, J. T., Shi, Q., Kolb, C. E., Worsnop, D. R., Yourshaw, I., Seinfeld, J. H., Flagan, R. C., Zhang, X. F., Smith, K. A., Morris, J. W., and Davidovits, P.: Ambient aerosol sampling using the Aerodyne Aerosol Mass Spectrometer, *J. Geophys. Res.*, 108, 8425, doi:10.1029/2001JD001213, 2003.
- Kanakidou, M., Seinfeld, J. H., Pandis, S. N., Barnes, I., Dentener, F. J., Facchini, M. C., Van Dingenen, R., Ervens, B., Nenes, A., Nielsen, C. J., Swietlicki, E., Putaud, J. P., Balkanski, Y., Fuzzi, S., Horth, J., Moortgat, G. K., Winterhalter, R., Myhre, C. E. L., Tsigaridis, K., Vignati, E., Stephanou, E. G., and Wilson, J.: Organic aerosol and global climate modelling: a review, *Atmos. Chem. Phys.*, 5, 1053–1123, doi:10.5194/acp-5-1053-2005, 2005.
- Katen, P. C. and Hubbe, J. M.: An evaluation of optical-particle counter measurements of the dry deposition of atmospheric aerosol-particles, *J. Geophys. Res.*, 90, 2145–2160, 1985.
- Kimmel, J. R., Farmer, D. K., Cubison, M. J., Sueper, D., Tanner, C., Nemitz, E., Worsnop, D. R., Gonin, M., and Jimenez, J. L.: Real-time aerosol mass spectrometry with millisecond resolution, *Int. J. Mass Spectrom.*, in press, December, 2010.
- Lamanna, M. S. and Goldstein, A. H.: In situ measurements of C-2–C-10 volatile organic compounds above a Sierra Nevada ponderosa pine plantation, *J. Geophys. Res.*, 104, 21247–21262, 1999.
- Lindberg, S. E., Lovett, G. M., Richter, D. D., and Johnson, D. W.: Atmospheric deposition and canopy interactions of major ions in a forest, *Science*, 231, 141–145, 1986.
- Magill, A. H., Aber, J. D., Currie, W. S., Nadelhoffer, K. J., Martin, M. E., McDowell, W. H., Melillo, J. M., and Steudler, P.: Ecosystem response to 15 years of chronic nitrogen additions at the Harvard Forest LTER, Massachusetts, USA, *Forest Ecol. Manage.*, 196, 7–28, 2004.
- Magnani, F., Mencuccini, M., Borghetti, M., Berbigier, P., Berninger, F., Delzon, S., Grelle, A., Hari, P., Jarvis, P. G., Kolari, P., Kowalski, A. S., Lankreijer, H., Law, B. E., Lindroth, A., Lous-tau, D., Manca, G., Moncrieff, J. B., Rayment, M., Tedeschi, V., Valentini, R., and Grace, J.:

**Eddy covariance  
HR-AMS aerosol  
fluxes**

D. K. Farmer et al.

[Title Page](#)[Abstract](#)[Introduction](#)[Conclusions](#)[References](#)[Tables](#)[Figures](#)[◀](#)[▶](#)[◀](#)[▶](#)[Back](#)[Close](#)[Full Screen / Esc](#)[Printer-friendly Version](#)[Interactive Discussion](#)

The human footprint in the carbon cycle of temperate and boreal forests, *Nature*, 447, 848–850, 2007.

Mårtensson, E. M., Nilsson, E. D., Buzorius, G., and Johansson, C.: Eddy covariance measurements and parameterisation of traffic related particle emissions in an urban environment, *Atmos. Chem. Phys.*, 6, 769–785, doi:10.5194/acp-6-769-2006, 2006.

Martin, R. V., Jacob, D. J., Yantosca, R. M., Chin, M., and Ginoux, P.: Global and regional decreases in tropospheric oxidants from photochemical effects of aerosols, *J. Geophys. Res.*, 108, 4097, doi:10.1029/2002JD002622, 2003.

Matson, P., Lohse, K. A., and Hall, S. J.: The globalization of nitrogen deposition: consequences for terrestrial ecosystems, *Ambio*, 31, 113–119, 2002.

Misson, L., Tang, J. W., Xu, M., McKay, M., and Goldstein, A.: Influences of recovery from clear-cut, climate variability, and thinning on the carbon balance of a young ponderosa pine plantation, *Agr. Forest Meteorol.*, 130, 207–222, 2005.

Monks, P. S., Granier, C., Fuzzi, S., Stohl, A., Williams, M. L., Akimoto, H., Amann, M., Baklanov, A., Baltensperger, U., Bey, I., Blake, N., Blake, R. S., Carslaw, K., Cooper, O. R., Dentener, F., Fowler, D., Fragkou, E., Frost, G. J., Generoso, S., Ginoux, P., Grewe, V., Guenther, A., Hansson, H. C., Henne, S., Hjorth, J., Hofzumahaus, A., Huntrieser, H., Isaksen, I. S. A., Jenkin, M. E., Kaiser, J., Kanakidou, M., Klimont, Z., Kulmala, M., Laj, P., Lawrence, M. G., Lee, J. D., Liousse, C., Maione, M., McFiggans, G., Metzger, A., Mieville, A., Moussiopoulos, N., Orlando, J. J., O'Dowd, C. D., Palmer, P. I., Parrish, D. D., Petzold, A., Platt, U., Pöschl, U., Prévôt, A. S. H., Reeves, C. E., Reimann, S., Rudich, Y., Sellegri, K., Steinbrecher, R., Simpson, D., ten Brink, H., Theloke, J., van der Werf, G. R., Vautard, R., Vestreng, V., Vlachokostas, C., and von Glasow, R.: Atmospheric composition change – global and regional air quality, *Atmos. Environ.*, 43, 5268–5350, 2009.

Müller, M., Graus, M., Ruuskanen, T. M., Schnitzhofer, R., Bamberger, I., Kaser, L., Titzmann, T., Hörtnagl, L., Wohlfahrt, G., Karl, T., and Hansel, A.: First eddy covariance flux measurements by PTR-TOF, *Atmos. Meas. Tech.*, 3, 387–395, doi:10.5194/amt-3-387-2010, 2010.

Murphy, J. G., Day, D. A., Cleary, P. A., Wooldridge, P. J., and Cohen, R. C.: Observations of the diurnal and seasonal trends in nitrogen oxides in the western Sierra Nevada, *Atmos. Chem. Phys.*, 6, 5321–5338, doi:10.5194/acp-6-5321-2006, 2006.

Myles, L., Meyers, T. P., and Robinson, L.: Relaxed eddy accumulation measurements of ammonia, nitric acid, sulfur dioxide and particulate sulfate dry deposition near Tampa, FL, USA, *Environ. Res. Lett.*, 2, 034004, doi:10.1088/1748-9326/2/3/034004, 2007.

**Eddy covariance  
HR-AMS aerosol  
fluxes**

D. K. Farmer et al.

Title Page

Abstract

Introduction

Conclusions

References

Tables

Figures

◀

▶

◀

▶

Back

Close

Full Screen / Esc

Printer-friendly Version

Interactive Discussion



Nemitz, E., Sutton, M. A., Wyers, G. P., and Jongejan, P. A. C.: Gas-particle interactions above a Dutch heathland: I. Surface exchange fluxes of  $\text{NH}_3$ ,  $\text{SO}_2$ ,  $\text{HNO}_3$  and HCl, *Atmos. Chem. Phys.*, 4, 989–1005, doi:10.5194/acp-4-989-2004, 2004a.

5 Nemitz, E., Sutton, M. A., Wyers, G. P., Otjes, R. P., Mennen, M. G., van Putten, E. M., and Gallagher, M. W.: Gas-particle interactions above a Dutch heathland: II. Concentrations and surface exchange fluxes of atmospheric particles, *Atmos. Chem. Phys.*, 4, 1007–1024, doi:10.5194/acp-4-1007-2004, 2004b.

10 Nemitz, E., Jimenez, J. L., Huffman, J. A., Ulbrich, I. M., Canagaratna, M. R., Worsnop, D. R., and Guenther, A. B.: An eddy-covariance system for the measurement of surface/atmosphere exchange fluxes of submicron aerosol chemical species – first application above an urban area, *Aerosol Sci. Tech.*, 42, 636–657, 2008.

Nemitz, E., Dorsey, J. R., Flynn, M. J., Gallagher, M. W., Hensen, A., Erismann, J.-W., Owen, S. M., Dämmgen, U., and Sutton, M. A.: Aerosol fluxes and particle growth above managed grassland, *Biogeosciences*, 6, 1627–1645, doi:10.5194/bg-6-1627-2009, 2009a.

15 Nemitz, E., Hargreaves, K. J., Neftel, A., Loubet, B., Cellier, P., Dorsey, J. R., Flynn, M., Hensen, A., Weidinger, T., Meszaros, R., Horvath, L., Dämmgen, U., Frühauf, C., Löpmeier, F. J., Gallagher, M. W., and Sutton, M. A.: Intercomparison and assessment of turbulent and physiological exchange parameters of grassland, *Biogeosciences*, 6, 1445–1466, doi:10.5194/bg-6-1445-2009, 2009b.

20 Pett-Ridge, J. C.: Contributions of dust to phosphorus cycling in tropical forests of the Luquillo Mountains, Puerto Rico, *Biogeochemistry*, 94, 63–80, 2009.

Rowe, M. D., Fairall, C. W., and Perlinger, J. A.: Chemical sensor resolution requirements for near-surface measurements of turbulent fluxes, *Atmos. Chem. Phys. Discuss.*, 10, 24409–24433, doi:10.5194/acpd-10-24409-2010, 2010.

25 Ruijgrok, W., Tieben, H., and Eisinga, P.: The dry deposition of particles to a forest canopy: a comparison of model and experimental results, *Atmos. Environ.*, 31, 399–415, 1997.

Sievering, H.: Small-particle dry deposition under high wind-speed conditions – eddy flux measurements at the Boulder-Atmospheric-Observatory, *Atmos. Environ.*, 21, 2179–2185, 1987.

30 Stein, S. E.: “Mass Spectra” in NIST Chemistry WebBook, NIST Standard Reference Database Number 69, edited by: Linstrom, P. J. and Mallard, W. G., National Institute of Standards and Technology, Gaithersburg MD, available at: <http://webbook.nist.gov>, 20899, last access: 5 June, 2010.

**Eddy covariance  
HR-AMS aerosol  
fluxes**

D. K. Farmer et al.

[Title Page](#)[Abstract](#)[Introduction](#)[Conclusions](#)[References](#)[Tables](#)[Figures](#)[◀](#)[▶](#)[◀](#)[▶](#)[Back](#)[Close](#)[Full Screen / Esc](#)[Printer-friendly Version](#)[Interactive Discussion](#)

- Stevens, C. J., Dise, N. B., Mountford, J. O., and Gowing, D. J.: Impact of nitrogen deposition on the species richness of grasslands, *Science*, 303, 1876–1879, 2004.
- Sun, Y. and Zhang, Q.: Bulk characterization and quantification of organic nitrogen species in atmospheric condensed phases based on high resolution time-of-flight Aerosol Mass Spectrometry, *Environ. Sci. Technol.*, in preparation, 2010.
- Sutton, M. A., Simpson, D., Levy, P. E., Smith, R. I., Reis, S., van Oijen, M., and de Vries, W.: Uncertainties in the relationship between atmospheric nitrogen deposition and forest carbon sequestration, *Global Change Biol.*, 14, 2057–2063, 2008.
- Taipale, R., Ruuskanen, T. M., and Rinne, J.: Lag time determination in DEC measurements with PTR-MS, *Atmos. Meas. Tech.*, 3, 853–862, doi:10.5194/amt-3-853-2010, 2010.
- Textor, C., Schulz, M., Guibert, S., Kinne, S., Balkanski, Y., Bauer, S., Berntsen, T., Berglen, T., Boucher, O., Chin, M., Dentener, F., Diehl, T., Easter, R., Feichter, H., Fillmore, D., Ghan, S., Ginoux, P., Gong, S., Grini, A., Hendricks, J., Horowitz, L., Huang, P., Isaksen, I., Iversen, I., Kloster, S., Koch, D., Kirkevåg, A., Kristjansson, J. E., Krol, M., Lauer, A., Lamarque, J. F., Liu, X., Montanaro, V., Myhre, G., Penner, J., Pitari, G., Reddy, S., Seland, Ø., Stier, P., Takemura, T., and Tie, X.: Analysis and quantification of the diversities of aerosol life cycles within AeroCom, *Atmos. Chem. Phys.*, 6, 1777–1813, doi:10.5194/acp-6-1777-2006, 2006.
- Thomas, R. M., Trebs, I., Otjes, R., Jongejan, P. A. C., Ten Brink, H., Phillips, G., Kortner, M., Meixner, F. X., and Nemitz, E.: An automated analyzer to measure surface-atmosphere exchange fluxes of water soluble inorganic aerosol compounds and reactive trace gases, *Environ. Sci. Technol.*, 43, 1412–1418, 2009.
- Trebs, I., Lara, L. L., Zeri, L. M. M., Gatti, L. V., Artaxo, P., Dlugi, R., Slanina, J., Andreae, M. O., and Meixner, F. X.: Dry and wet deposition of inorganic nitrogen compounds to a tropical pasture site (Rondônia, Brazil), *Atmos. Chem. Phys.*, 6, 447–469, doi:10.5194/acp-6-447-2006, 2006.
- Vicars, W. C., Sickman, J. O., and Ziemann, P. J.: Atmospheric phosphorus deposition at a montane site: Size distribution, effects of wildfire, and ecological implications, *Atmos. Environ.*, 44, 2813–2821, 2010.
- Vitousek, P. M. and Howarth, R. W.: Nitrogen limitation on land and in the sea – how can it occur, *Biogeochemistry*, 13, 87–115, 1991.
- Vong, R. J., Vong, I. J., Vickers, D., and Covert, D. S.: Size-dependent aerosol deposition velocities during BEARPEX'07, *Atmos. Chem. Phys.*, 10, 5749–5758, doi:10.5194/acp-10-5749-2010, 2010.

**Eddy covariance  
HR-AMS aerosol  
fluxes**

D. K. Farmer et al.

[Title Page](#)[Abstract](#)[Introduction](#)[Conclusions](#)[References](#)[Tables](#)[Figures](#)[⏪](#)[⏩](#)[◀](#)[▶](#)[Back](#)[Close](#)[Full Screen / Esc](#)[Printer-friendly Version](#)[Interactive Discussion](#)

- Webb, E. K., Pearman, G. I., and Leuning, R.: Correction of flux measurements for density effects due to heat and water-vapor transfer, *Q. J. Roy. Meteor. Soc.*, 106, 85–100, 1980.
- Wesely, M. L. and Hicks, B. B.: A review of the current status of knowledge on dry deposition, *Atmos. Environ.*, 34, 2261–2282, 2000.
- 5 Wienhold, F. G., Welling, M., and Harris, G. W.: Micrometeorological measurement and source region analysis of nitrous-oxide fluxes from an agricultural soil, *Atmos. Environ.*, 29, 2219–2227, 1995.
- 10 Wolff, V., Trebs, I., Foken, T., and Meixner, F. X.: Exchange of reactive nitrogen compounds: concentrations and fluxes of total ammonium and total nitrate above a spruce canopy, *Biogeosciences*, 7, 1729–1744, doi:10.5194/bg-7-1729-2010, 2010.

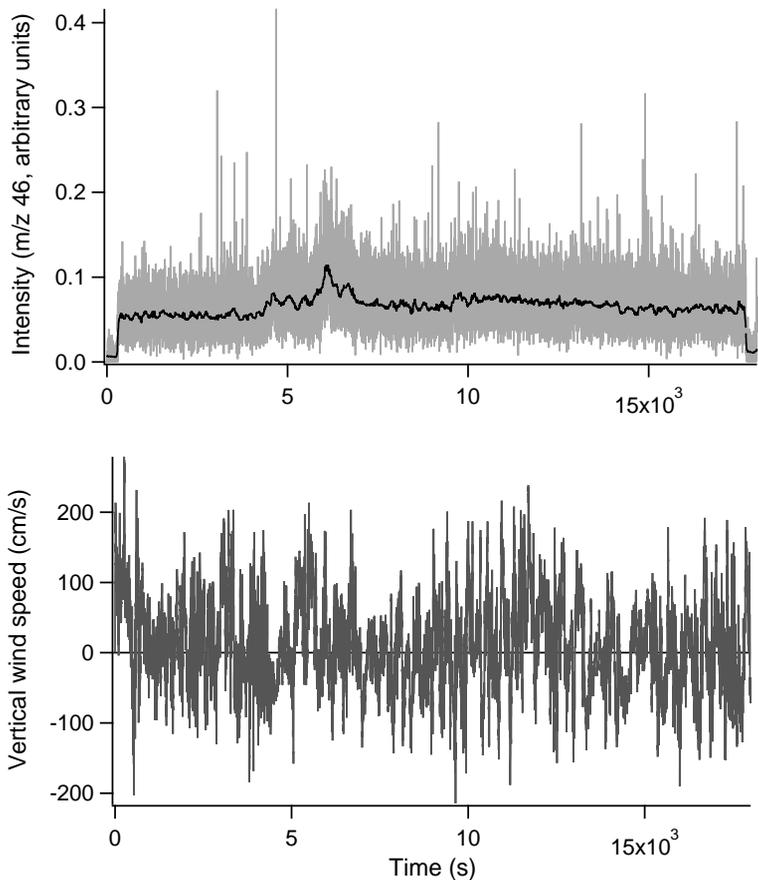


**Fig. 1.** A complete 30 min flux cycle of vertical wind speed and the UR  $m/z$  46 signal acquired at 10 Hz between 04:00–04:30 p.m., 7 September 2007. The first and final 30 s represent the gas+background signal, while the intervening 29 min represent the aerosol+gas+background transmitted signal. The black line is the 100 point (10 s) running mean.

**Eddy covariance  
HR-AMS aerosol  
fluxes**

D. K. Farmer et al.

Title Page

Abstract

Introduction

Conclusions

References

Tables

Figures

◀

▶

◀

▶

Back

Close

Full Screen / Esc

Printer-friendly Version

Interactive Discussion



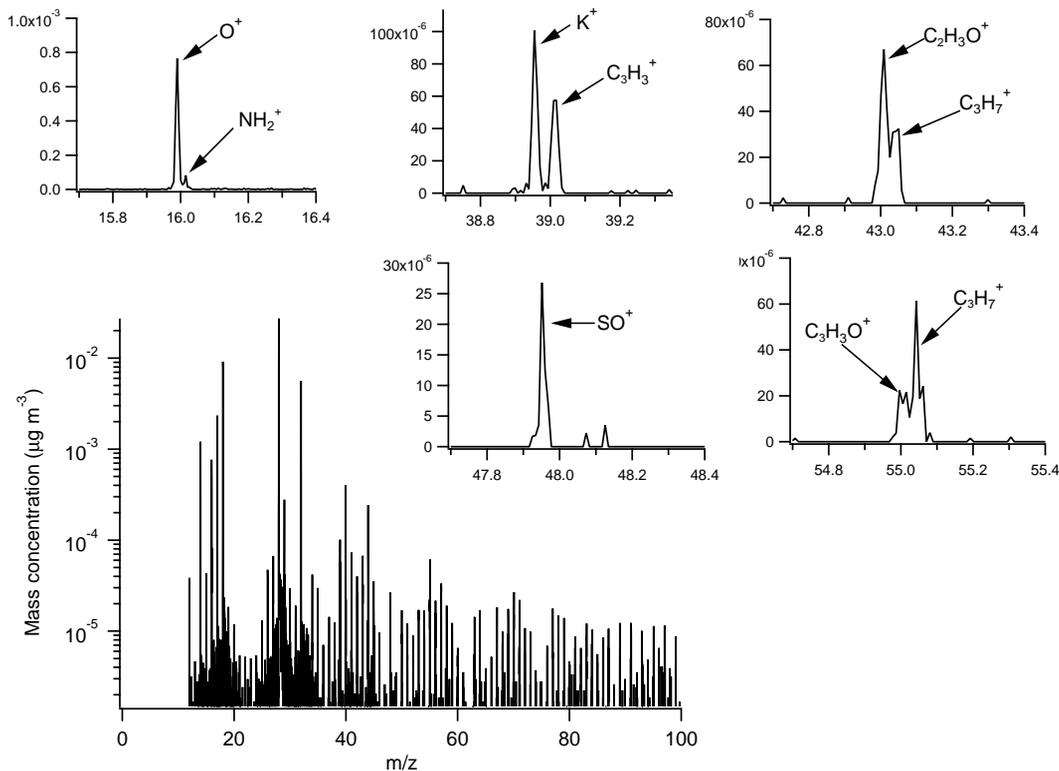


**Fig. 2.** The particle and gas phase mass spectrum, in  $\text{NO}_3\text{-eq } \mu\text{g m}^{-3}$ , was taken on 7 September 2007 and calculated from a 0.0925 s average of ambient data collected in the transmitted (aerosol + gas + AMS background) minus the average gas+AMS background mass spectra. The insets show the mass spectrum around  $m/z$  16, 39, 43, 48 and 55.

**Eddy covariance  
HR-AMS aerosol  
fluxes**

D. K. Farmer et al.

Title Page

Abstract

Introduction

Conclusions

References

Tables

Figures

◀

▶

◀

▶

Back

Close

Full Screen / Esc

Printer-friendly Version

Interactive Discussion



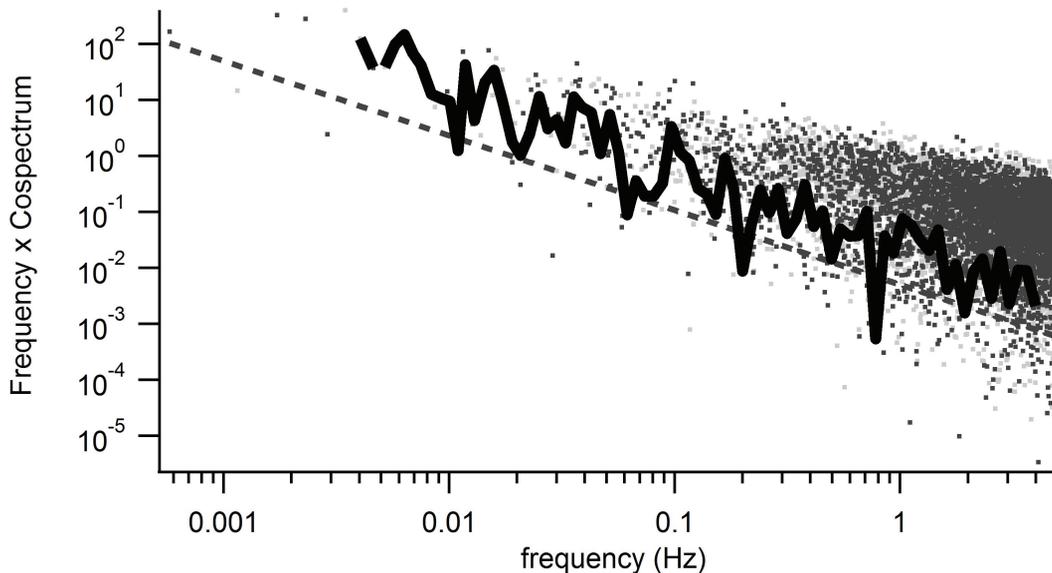


**Fig. 3.** Frequency-multiplied co-spectrum of the HR  $\text{NH}_2^+$  fragment for a single half hour, acquired at 10 Hz between 04:00–04:30 p.m., 7 September 2007. Positive data points are indicated by light grey dots, negative by dark grey dots. As the average  $\text{NH}_3^+$  flux is downwards, negative points dominate the co-spectrum. The solid black line is a binned average of all the data, while the dashed black line follows the  $-4/3$  slope characteristic of the inertial turbulence sub-range.

**Eddy covariance  
HR-AMS aerosol  
fluxes**

D. K. Farmer et al.

Title Page

Abstract

Introduction

Conclusions

References

Tables

Figures

◀

▶

◀

▶

Back

Close

Full Screen / Esc

Printer-friendly Version

Interactive Discussion



Eddy covariance  
HR-AMS aerosol  
fluxes

D. K. Farmer et al.

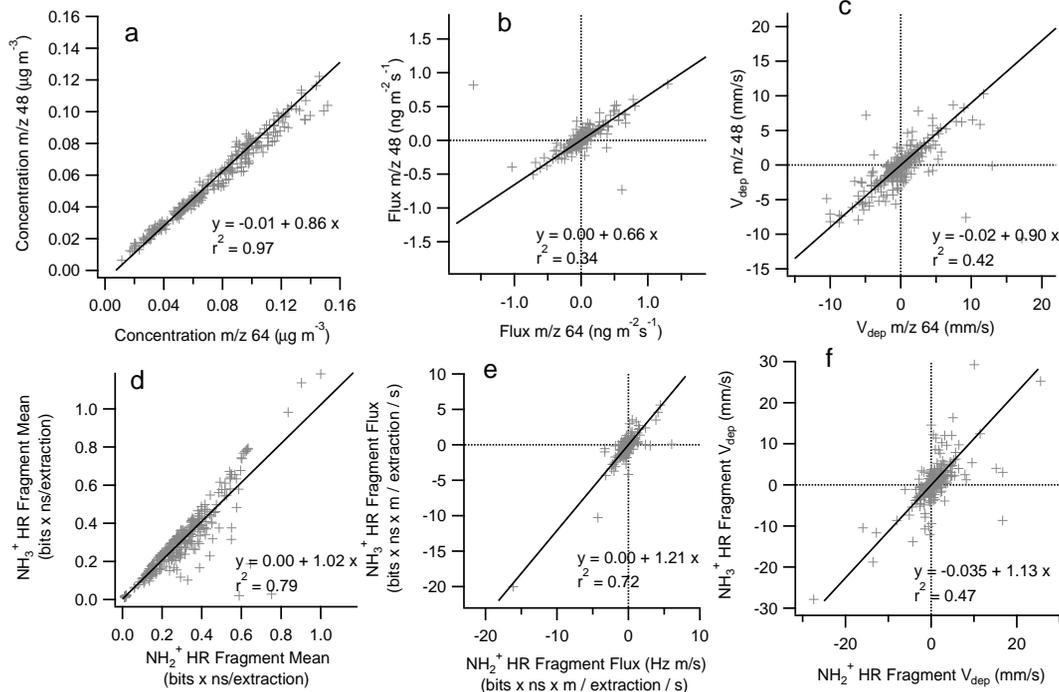


**Fig. 4.** Comparisons of mean mass concentration (or signal), flux and deposition velocity for sulphate-dominated UR  $m/z$  48 and 64 (**a–c**) and high resolution fragments  $\text{NH}_2^+$  and  $\text{NH}_3^+$  (**d–f**). Linear regressions are calculated with a weighted robust regression to account for uncertainties in both  $x$  and  $y$  directions, with the exception of ammonium deposition velocity (**f**), for which we use a weighted orthogonal distance regression.

Title Page

Abstract

Introduction

Conclusions

References

Tables

Figures

◀

▶

◀

▶

Back

Close

Full Screen / Esc

Printer-friendly Version

Interactive Discussion



## Eddy covariance HR-AMS aerosol fluxes

D. K. Farmer et al.

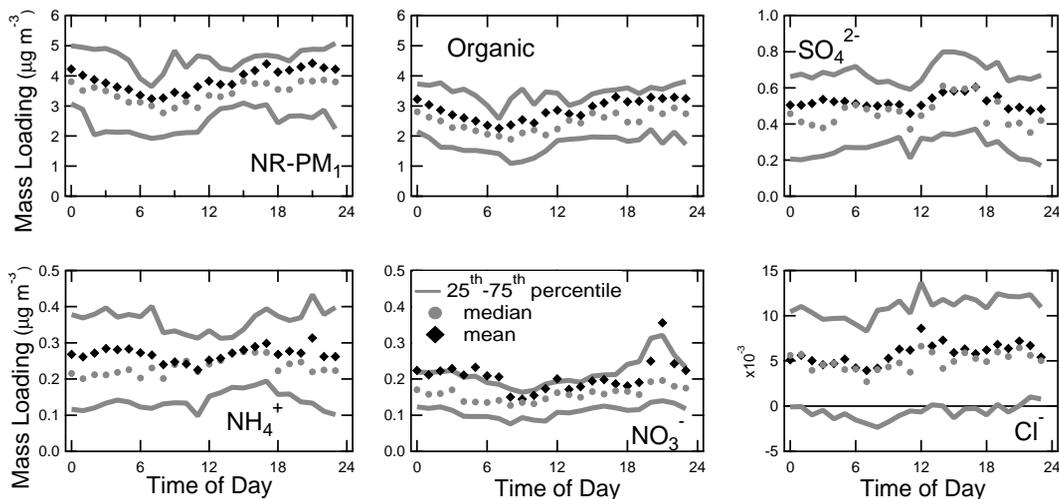


**Fig. 5.** Diurnal cycles for mass concentrations of total NR-PM<sub>1</sub> and the organic, ammonium, nitrate, sulphate, and chloride components for the entire BEARPEX-2007 campaign (18 August 2007–2 October 2007). Hourly means and medians are shown in black diamonds and grey circles, respectively; grey lines indicate the 25th and 75th percentiles.

[Title Page](#)
[Abstract](#)
[Introduction](#)
[Conclusions](#)
[References](#)
[Tables](#)
[Figures](#)
[Back](#)
[Close](#)
[Full Screen / Esc](#)
[Printer-friendly Version](#)
[Interactive Discussion](#)


**Eddy covariance  
HR-AMS aerosol  
fluxes**

D. K. Farmer et al.

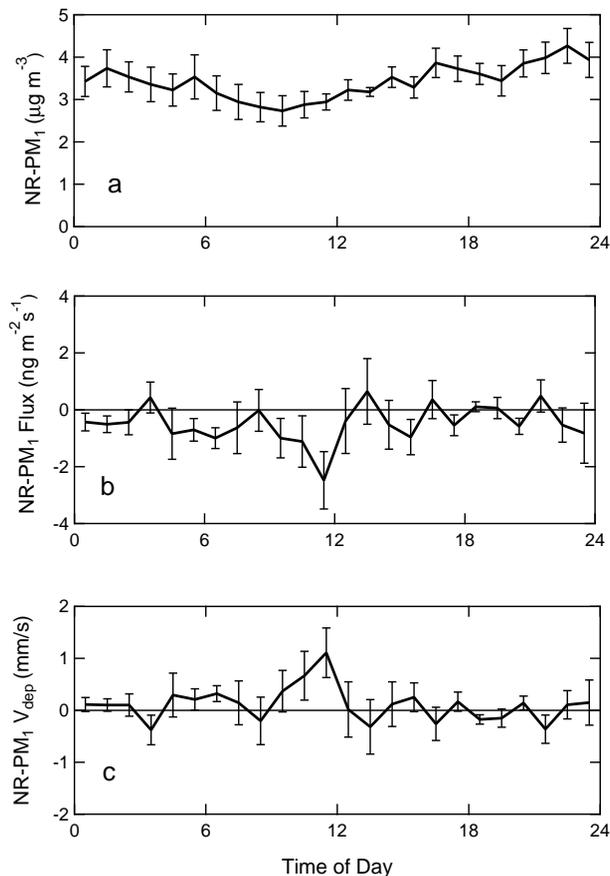


**Fig. 6.** Diurnal cycles of mass concentrations, fluxes and deposition velocities of total NR-PM<sub>1</sub> mass from flux data for 13–27 September 2007. Uncertainties are taken as the standard error of the mean for each time bin.

[Title Page](#)[Abstract](#)[Introduction](#)[Conclusions](#)[References](#)[Tables](#)[Figures](#)[◀](#)[▶](#)[◀](#)[▶](#)[Back](#)[Close](#)[Full Screen / Esc](#)[Printer-friendly Version](#)[Interactive Discussion](#)

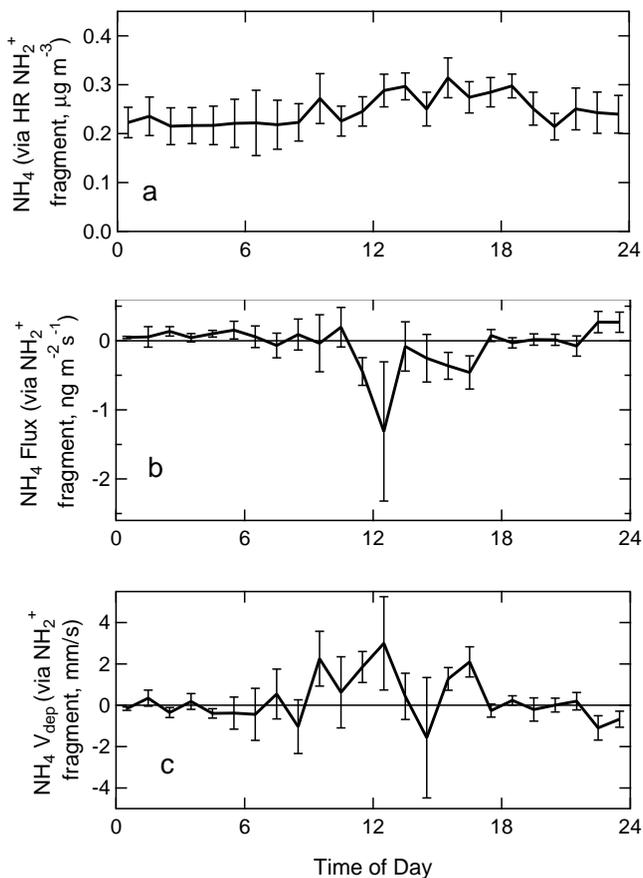


**Fig. 7.** Diurnal cycles of mass concentrations, fluxes and deposition velocities of particulate ammonium, as calculated from the  $\text{NH}_2^+$  HR fragment from fast, flux data for 13–27 September 2007. Uncertainties are taken as the standard error of the mean for each time bin.

**Eddy covariance  
HR-AMS aerosol  
fluxes**

D. K. Farmer et al.

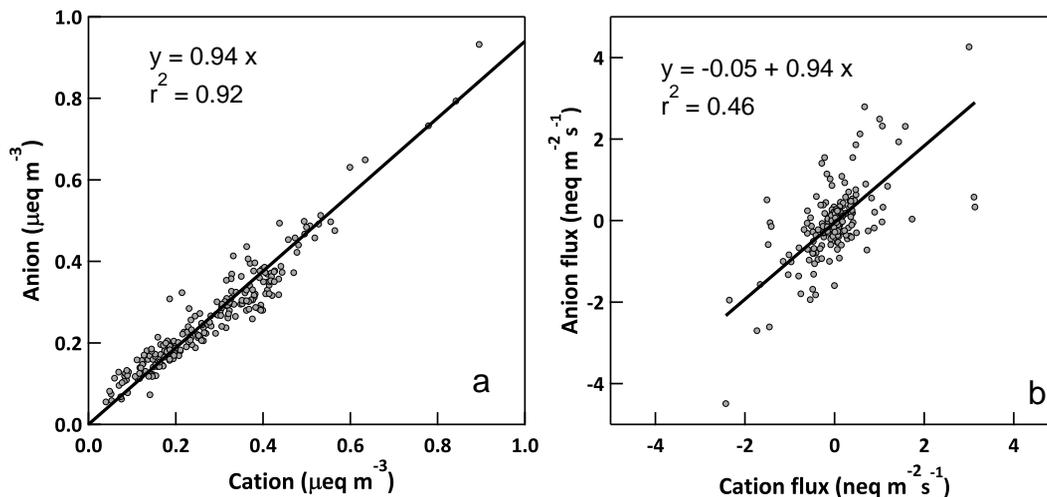


**Fig. 8.** The acid balance for NR-PM<sub>1</sub> aerosol: comparison of concentrations and fluxes for cations (ammonium) versus anions (sulphate, nitrate, chloride). The solid lines are the robust regression fits. Note that the regression for cation and anion concentrations forces a zero intercept because the zero of these components are verified by periods in which ambient air is sampled through a total particle filter, and should not have an offset with respect to each other.

[Title Page](#)[Abstract](#)[Introduction](#)[Conclusions](#)[References](#)[Tables](#)[Figures](#)[⏪](#)[⏩](#)[◀](#)[▶](#)[Back](#)[Close](#)[Full Screen / Esc](#)[Printer-friendly Version](#)[Interactive Discussion](#)